

Formation of phosphorus monobromide (PBr) and phosphorus monoiodide (PI) radicals through direct radiative association: Prospects for astrochemical environments

Qinghui Wei(魏庆卉), Yang Chen(陈扬), Amaury A. de Almeida, Carmen M. Andreazza, Hongjing Liang(梁红静), and Bing Yan(闫冰)

Citation: Chin. Phys. B, 2026, 35 (**3**): 033301. DOI: 10.1088/1674-1056/adfdc7
http://cpb.iphy.ac.cn; http://iopscience.iop.org/cpb

What follows is a list of articles you may be interested in

Optical spectroscopy of CrO and electronic states of the Cr group metal monoxides

Lei Zhang(张磊), Yao Yu(于尧), Xinwen Ma(马新文), and Jie Yang(杨杰)
Chin. Phys. B, 2023, 32 (**5**): 053301. DOI: 10.1088/1674-1056/acb763

Spectroscopic study of $B^2\Sigma^+$–$X_1\ ^2\Pi_{1/2}$ transition of electron electric dipole moment candidate PbF

Ben Chen(陈犇), Yi-Ni Chen(陈旖旎), Jia-Nuan Pan(潘佳煖), Jian-Ping Yin(印建平), and Hai-Ling Wang(汪海玲)†
Chin. Phys. B, 2022, 31 (**9**): 093301. DOI: 10.1088/1674-1056/ac633a

Line positions, intensities, and Einstein *A* coefficients for 3-0 band of $^{12}C^{16}O$: A spectroscopy learning method

Zhi-Xiang Fan(范志祥), Zhi-Zhang Ni(倪志樟), Jie-Jie He(贺洁洁), Yi-Fan Wang(王一凡), Qun-Chao Fan(樊群超), Jia Fu(付佳), Yong-Gen Xu(徐勇根), Hui-Dong Li(李会东), Jie Ma(马杰), and Feng Xie(谢锋)
Chin. Phys. B, 2021, 30 (**12**): 123301. DOI: 10.1088/1674-1056/ac3069

R-branch high-lying transition emission spectra of SbNa molecule

Chun-Run Luo(罗春润), Qun-Chao Fan(樊群超), Zhi-Xiang Fan(范志祥), Jia Fu(付佳), Jie Ma(马杰), Hui-Dong Li(李会东), and Yong-Gen Xu(徐勇根)
Chin. Phys. B, 2021, 30 (**1**): 013301. DOI: 10.1088/1674-1056/abc3b2

Study on the $A^2\Pi_{3/2u}$, $B^2\Delta_{3/2u}$, and $X^2\Pi_{3/2g}$ states of Cl_2^+ including its isotopologues

Wu Ling (吴玲), You Su-Ping (尤素萍), Shao Xu-Ping (邵旭萍), Chen Gang-Jin (陈钢进), Ding Ning (丁宁), Wang You-Mei (汪友梅), Yang Xiao-Hua (杨晓华)
Chin. Phys. B, 2015, 24 (**8**): 083301. DOI: 10.1088/1674-1056/24/8/083301

Formation of phosphorus monobromide (PBr) and phosphorus monoiodide (PI) radicals through direct radiative association: Prospects for astrochemical environments

Qinghui Wei(魏庆卉)[1], Yang Chen(陈扬)[1], Amaury A. de Almeida[2], Carmen M. Andreazza[3], Hongjing Liang(梁红静)[1,4,†], and Bing Yan(闫冰)[1,‡]

[1] *Institute of Atomic and Molecular Physics, Jilin University, Changchun* 130012, *China*
[2] *Instituto de Astronomia, Geofísica e Ciências Atmosféricas, Universidade de São Paulo, Rua do Matão* 1226, 05508-090, *São Paulo, SP, Brazil*
[3] *Instituto de Geoci.encias e Ci.encias Exatas, Universidade Estadual Paulista, Av.* 24*A*, 13506-900, *Rio Claro SP, Brazil*
[4] *College of Science, Jilin Institute of Chemical Technology, Jilin* 132022, *China*

(Received 13 June 2025; revised manuscript received 21 July 2025; accepted manuscript online 21 August 2025)

The cross sections and rate constants for the formation of phosphorus monobromide (PBr) and phosphorus monoiodide (PI) radicals through radiative association have been theoretically estimated using fully quantum mechanical methods. For temperatures ranging from 10 K to 15000 K, the thermal rate coefficients are found to vary from 2.86×10^{-23} $cm^3\cdot s^{-1}$ to 1.20×10^{-18} $cm^3\cdot s^{-1}$ and from 7.73×10^{-24} $cm^3\cdot s^{-1}$ $cm^3\cdot s^{-1}$ to 1.12×10^{-18} $cm^3\cdot s^{-1}$ for PBr and PI, respectively. Implications of PBr and PI radiative association to various astrochemical environments are briefly discussed.

Keywords: PBr and PI radicals, radiative association, molecular data, molecular process

PACS: 33.20.Vq, 34.50.Cx, 98.38.Bn, 95.30.Ft

DOI: 10.1088/1674-1056/adfdc7 **CSTR:** 32038.14.CPB.adfdc7

1. Introduction

Despite the low solar elemental abundances of bromine and iodine (number ratios [Br/H] = 3.5×10^{-10} and [I/H] = 3.6×10^{-11}, established from meteoritic sample analyses[1]), atomic lines of I and Br, as well I_2, IO, Br_2, BrO, HOBr and five short-lived brominated molecules (CH_2Br_2, $CHBr_3$, CH_2IBr, $CHCl_2Br$ and $CHClBr_2$) have all been identified in the atmosphere of Earth (e.g. Refs. [2–4], and the references therein). Furthermore, HBr was confirmed *in situ* in the inner coma of comet 67P/Churyumov-Gerimenko (67P/C-G) by Dhooghe *et al.*[5] However, HBr was not found in molecular clouds such as Orion KL, Sgr B2(N), and NGC 6334I with the Herschel/HUFI spectrometer by Ligterink and Kama.[6] Additionally, searches for the HBr^+ ion have also been conducted toward Orion KL, Sgr B2(N), and NGC 6334I molecular clouds,[6] but with negative results.

Outside the Solar System, lines from I^{4+} and I^{5+} ions have been measured in the ultraviolet (UV) spectra of white dwarf atmospheres, with abundance up to about 4 dex compared with solar value.[7–11] In turn, neutral bromine has been detected in the visual region of the spectrum of the very peculiar star HD101065 (Przybylski's star) by Bidelman.[12] Br^+ ion lines have been identified in the optical spectra of the ultra-peculiar (HgMn) star HR 7143,[13] and in the He-weak chemical peculiar star 3CenA[14] with bromine excesses of 2.3 and 2.6 dex over solar abundance, respectively. Faint optical line of Br_2^+ ion has been observed in the planetary nebulae,[15,16] with an approximated atomic Br abundance of [Br/H] = 3.39×10^{-9} from a possible blended line.[16] Near-infrared emission lines of Br^{3+} and Br^{4+} ions have been additionally seen in the spectra of planetary nebulae, with an abundance of [Br/H] = 0.10±0.10 relative to the solar value.[17] Still, Br^{4+} and Br^{5+} ions lines have been detected in the UV spectra of white dwarf atmospheres, revealing high quantities of atomic Br up to about 3 dex over solar abundance.[11,18]

Phosphorus compounds have been identified in the dust component of comets 67P/C-G,[19] 81P/Wild 2,[20] and 1P/Halley[21] and is habitual constituent in iron meteorites, particularly in the form of schreibersite ($(Ni,Fe)_3P$), apatite ($Ca_5(PO_4)_3(Cl,F,OH)$) and merrillite ($Ca_5NaMg(PO_4)_7$).[22] In the gas phase, P^+ ion lines have been detected in diffuse molecular clouds (e.g., Ref. [23]), in extragalactic objects,[24,25] supernova remnant Cas A,[26] and planetary nebulae.[16,25] Still, lines of atomic P have been observed in the comet 67P/C-G,[27,27] and towards dwarf[29] and giant stars.[30,31] In molecular form, six P-bearing molecules have been observed in the circumstellar envelope of evolved stars (PO, PN, CP, HCP, CCP, and PH_3),[32–38] and one (SiP) tentatively identified.[39] However, only PN, PO, and PO^+ have been identified in star-forming regions.[40–46] In addition, PN has been observed in extragalactic sources,[47] PH_3 has been

†Corresponding author. E-mail: lianghongjing@jlict.edu.cn
‡Corresponding author. E-mail: yanbing@jlu.edu.cn

© 2026 Chinese Physical Society and IOP Publishing Ltd. All rights, including for text and data mining, AI training, and similar technologies, are reserved.

detected in the atmospheres of Jupiter[48] and Saturn,[49] and PO has been identified in the comet 67P/C-G.[27,28]

Phosphorus plays a critical role in prebiotic chemistry (e.g., in DNA, RNA, and ATP). Besides phosphorus, bromine is also essential for collagen functions in animals and iodine is required for thyroid hormones in mammals (e.g., Ref. [50]). Phosphorus is believed to be mainly produced by neutron capture in massive stars ($\geqslant 8M_{\odot}$), which are then ejected into interstellar medium during supernova explosion.[26,51–55] Indeed, largely enhanced P^{+} ions have been measured in supernova remnant Cas A (e.g., Ref. [26]). However, core-collapse supernovae cannot explain some observed atomic P abundances derived from spectroscopic observations of stars (e.g., Refs. [29,30]). So, atomic P is also thought to be synthesized during the asymptotic giant branch (AGB) ($< 8M_{\odot}$),[25,56,57] as well in type Ia supernovae,[58,59] and novae[60,61] explosions. In turn, the production of bromine and iodine via neutron capture processes is expected to occur in massive stars shells, and during supernova and kilonova explosions (e.g., Refs. [54,62–64]), as well as during the AGB phase.[65,66]

The radiative association may be one of the earliest proposed molecular formation mechanisms in astronomical sources[67] and is currently thought to play a significant role in the formation of simple molecules in relatively hot and low-density astrophysical environments, where hydrogen is absent and the dust grains still have to be formed, such as carbon-rich Wolf–Rayet winds and ejecta of supernovae (e.g., Refs. [68–70] and references therein). Still, this process has been included in the chemical networks proposed for novae ejecta (e.g., Refs. [71,72]), fast neutral winds from protostars,[73] and inner regions of the circumstellar envelopes of AGBs (e.g., Ref. [74]), among others. All these astrophysical sources have temperatures of the order of 1500 K–6000 K.

Studies of Br-, I-, and P-compounds in space are particularly relevant due to their role in the context of biochemistry and to our understanding of the formation and chemical evolution of these compounds in astrophysical sources. However, the chemistry of these elements has never been clearly characterized and only a few rate coefficients have been documented, (e.g., Refs. [6,75]). Understanding how phosphorus interacts with halogens like bromine and iodine expands our knowledge of its chemical behavior in space. Hence, we considered in this work the radiative association (RA) of Br(^{2}P) and I(^{2}P) atoms with P(^{4}S) atom to form the diatomic radicals PBr and PI, respectively. These radicals have not yet been detected in celestial bodies. However, PBr and PI can be formed by radiative association in astrophysical environments where phosphorus, bromine and iodine are available in gas phase, mainly in the ejecta of supernovae, as well in the inner regions of the envelope of AGBs and planetary nebulae, among others, where Br, I, and P elements are found to be largely enhanced compared to solar abundances due to nucleosynthesis. Thus, using potential energy curves and transition dipole moments obtained from accurate *ab initio* calculations, the radiative association cross sections were determined using fully quantum mechanical methods. Subsequently, the rate coefficients were estimated for temperatures ranging from 10 K to 15000 K.

2. Method of calculation

The formation of diatomic molecules by radiative association can occur when the atomic species approach each other with a relative energy E in a particular molecular state, which can decay to a bound electronic state through the spontaneous emission of a photon. In this processes, the quantum mechanical radiative association cross section for an electronic transition can be computed using perturbation theory, (e.g., Refs. [76–78]) given by

$$\sigma_{\Lambda\to\Lambda'}(E) = \sum_{J,v'j'} \frac{64}{3}\frac{\pi^5}{(4\pi\varepsilon_0)k_i^2} \times \frac{f_\Lambda}{\lambda^3_{E\Lambda' Sv'J'}} S_{J\Lambda,J'\Lambda'} \left|M_{iEJ,fv'J'}\right|^2, \quad (1)$$

where, the sum is over initial partial waves with the angular momenta J, the final vibrational v', and the rotational J', $k_i = (\sqrt{2\mu E})/\hbar$ is the wave number of the scattering state, $\hbar$ is the Planck constant, μ is the reduced mass of the collision system, ε_0 is the vacuum permittivity, $\lambda_{E\Lambda' Sv'J'}$ is the wave length of emitted photon, $S_{J\Lambda,J'\Lambda'}$ is Hönl–London factor. For the $\Pi \to \Sigma^-$ transitions of PBr and PI radicals, the Hönl–London factors are $S_{J,J-1} = (J+1)/4$, $S_{J,J} = (2J+1)/4$, and $S_{J,J+1} = J/4$, respectively;[79] f_Λ is the probability of approach in the scattering state, and it can be calculated as

$$f_\Lambda = \frac{(2S_\Lambda+1)(2-S_{0,\Lambda})}{(2L_\mathrm{A}+1)(2S_\mathrm{A}+1)(2L_\mathrm{B}+1)(2S_\mathrm{B}+1)}, \quad (2)$$

where, L_A, S_A, L_B, and S_B represent the electronic orbital and spin angular momenta of the A and B atoms, respectively. S is the spin quantum number of the electronic state Λ. δ is the Kronecker delta, $\delta = 1$ if $\Lambda = 0$, otherwise it is 0. Further, $M_{iEJ,fv'J'}$ is given by the integral

$$M_{iEJ,fv'J'} = \left\langle \Psi^{\Lambda}_{JE}(R) \left| D_{\Lambda\Lambda'}(R) \right| \Psi^{\Lambda'}_{J'v'}(R) \right\rangle, \quad (3)$$

where $\Psi^{\Lambda}_{JE}(R)$ and $\Psi^{\Lambda'}_{J'v'}(R)$ are radial wavefunctions for the continuum and bound states, respectively. These wave functions were obtained by solving the one-dimensional radial Schrödinger equation on the *ab initio* potential energy curve using the Numerov numerical integration method. $D_{\Lambda\Lambda'}(R)$ is the dipole transition moment between Λ and Λ' electronic states as a function of the internuclear distance R.

When the radiation association cross section is determined, the thermal rate coefficient (in units $\mathrm{cm^{-3}\cdot s^{-1}}$) at a given temperature T can be obtained by integrating the cross

section over a Maxwellian velocity distribution $f(E,T)$, and can be expressed as

$$k(T) = \int_0^\infty v(E) f(E,T) \sigma_{\Lambda\to\Lambda'} \mathrm{d}x, \tag{4}$$

where $v(E)$ is the initial relative velocity of the colliding atoms, $\sigma_{\Lambda\to\Lambda'}$ is the cross section of the radiation association, and

$$f(E,T) = 2\sqrt{\frac{E}{\pi(k_\mathrm{B}T)^3}}\,\mathrm{e}^{-E/k_\mathrm{B}T}, \tag{5}$$

these two formulas allows one to write

$$k_{\Lambda\to\Lambda'}(T) = \sqrt{\frac{8}{\pi\mu(k_\mathrm{B}T)^3}}\int_0^\infty E\sigma_{\Lambda\to\Lambda'}(E)\,\mathrm{e}^{-E/k_\mathrm{B}T}\,\mathrm{d}E, \tag{6}$$

where k_B is the Boltzmann constant.

3. Results and discussion

3.1. The PECs and TDMs of Λ–S electronic states

For PI and PBr, there are four electronic states correlating to the lowest dissociation limits $\mathrm{P}(^4\mathrm{S})+\mathrm{I}(^2\mathrm{P})$ and $\mathrm{P}(^4\mathrm{S})+\mathrm{Br}(^2\mathrm{P})$, respectively, namely $^{3,5}\Sigma^-$ and $^{3,5}\Pi$. The quintet states are repulsive in nature.[80–82] Hence, the electronic transitions from the quintet states is expected to contribute little to the radiative association cross-section and are not considered here. Therefore, the radiative association from $\mathrm{P}(^4\mathrm{S})+\mathrm{I}(^2\mathrm{P})$ and $\mathrm{P}(^4\mathrm{S})+\mathrm{Br}(^2\mathrm{P})$ to form PBr and PI, respectively, is possible through the $1^3\Pi$ electronic state, which then radiates to the ground $\mathrm{X}^3\Sigma^-$ state according to the selection rule. The statistical weight of the $1^3\Pi-\mathrm{X}^3\Sigma^-$ transitions of PBr and PI is 1/4.

The potential energy curves (PECs) of the $1^3\Pi$ and $\mathrm{X}^3\Sigma^-$ states of PBr and PI and transition dipole moments connecting these states which are being used in the present work have been obtained theoretically by Zhang *et al.*[80–82] Accurate ab initio multi-reference configuration interaction method plus Davidson correction ($+Q$) has been employed for this purpose.[83] To compensate for the energy cutoff error induced by the finite excitation space and improve the accuracy of the potential energy curve, the Davidson correction ($+Q$) was introduced, as it effectively estimates the impact of higher-order excitations on energy. These data are obtained over a range of internuclear separation R from 1.5 Å to 6.0 Å and 1.9 Å to 6.0 Å for PBr and PI molecules, respectively (Figs. 1 and 2). The $1^3\Pi$ state of PBr exhibits a potential well at approximately 2.6 Å, and features a barrier with a height of 0.07102 a.u. around 2.85 Å. In contrast, the $1^3\Pi$ state of PI also shows a shallow potential well near 4.50 Å. However, for radiative association rate constants calculations, transition dipole moments and potential energy curves are needed over a large range of internuclear distances. Hence, we extrapolate the values of the total potential energy curve and transition dipole moment. For small distances ($R<1.5$ Å for PBr and $R<1.9$ Å for PI), the interaction energy is fitted to the usual form

$$V(R) = A\exp(-BR) + C, \tag{7}$$

where A, B, and C are fitting parameters. At large separations ($R>6.0$ Å), the PECs, which are usually associated with long-range Coulomb forces and van der Waals dispersion, can be fitted using the following function:[84]

$$V(R) = -\frac{C_5}{R^5} - \frac{C_6}{R^6} + V(R\to\infty), \tag{8}$$

where C is the fitting coefficient, which can be estimated by fixing the value of and keeping the dissociation limit constant using the calculated *ab initio* data. is the dipole–dipole dispersion (van der Waals) coefficient, which can be estimated using London's formula:[85]

$$C_6 = \frac{3}{2}\frac{I_\mathrm{P}I_{\mathrm{Br/I}}}{I_\mathrm{P}+I_\mathrm{B}r/I}\alpha_\mathrm{d}^\mathrm{P}\alpha_\mathrm{d}^{\mathrm{Br/I}}. \tag{9}$$

Here, I_P, I_Br, and I_I are the dissociation energies of P, Br, and I atoms respectively, and their values can be obtained from NIST atomic spectral data.[86] The static dipole polarizability of P, Br, and I atoms (atomic unit) are equal to 24.5,[87] 23,[88] and 36,[88] respectively. The cubic spline was used to interpolate the points of PECs.

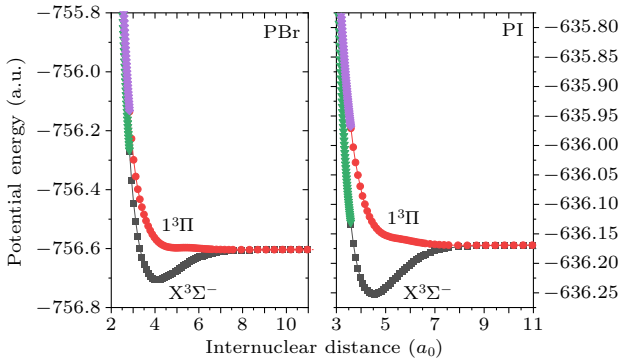


Fig. 1. The potential energy curves of PBr and PI. The green and purple parts are extrapolated and the black and red parts are taken from Zhang *et al.*[80–82]

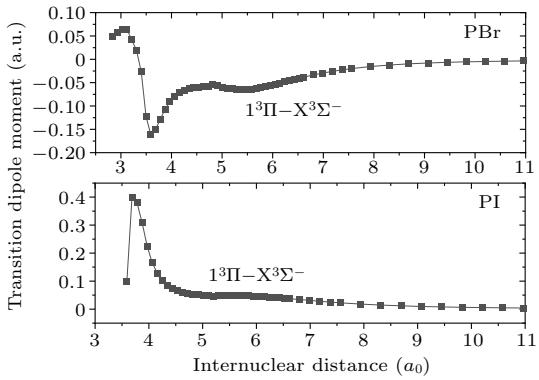


Fig. 2. Transition dipole moments of PBr and PI which are taken from Zhang *et al.*[80–82]

The radiative association cross sections for $1^3\Pi$–$X^3\Sigma^-$ transitions of PI and PBr are obtained using the quantum mechanical perturbation theory, which considers the contribution of the resonance. The results are shown in Fig. 3. It is clearly seen in this figure that the cross sections show a rather similar, at least qualitatively, energy dependence. When the energy is less than 10^{-2} eV, the computed cross sections markedly decrease as the collision energy increases. Above this energy, the cross sections increase rapidly due to the small potential barrier on the $1^3\Pi$ electronic state of PBr and PI. Finally, when the energy is greater than 2 eV, the cross sections show a sharp downward trend, due to Franck–Condon principle. In addition, several resonances are evident in the low energy region, especially at energies less than 10^{-2} eV, this type of resonance is usually a shape resonance, arising from a quasi-bound state supported by the effective potential of the initial electronic state, given by $V_{\rm eff}^{\rm A}(R) = V_{\rm A}(R) + \frac{J(J+1)}{2\mu R^2}$, where $V_{\rm A}(R)$ is negative. As J increases, $V_{\rm eff}^{\rm A}(R)$ decreases, the resonance peak will gradually decrease. Due to the potential barrier, tunneling rates will slow down, ultimately leading to resonance disappearance. At energies greater than 10^{-2} eV, because $1^3\Pi$ is a shallowly bound state, there is little resonance in this energy range. When rotational quantum number J increases, the absolute value of $V_{\rm eff}^{\rm A}(R)$ decreases gradually and the resonance structures disappear. In general, the radiative association cross sections of PBr are always larger than that of PI.

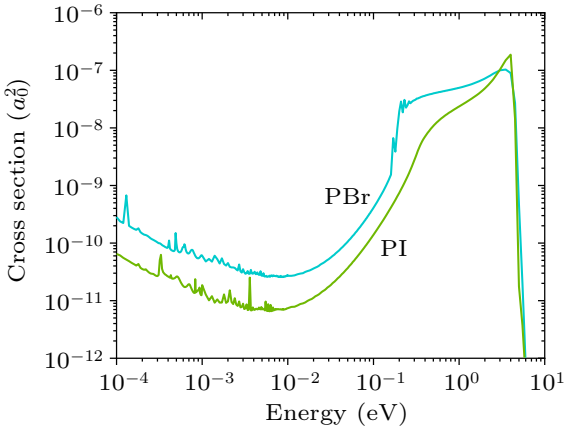


Fig. 3. Radiative association cross section of PBr and PI.

The radiative association rate coefficients values for PX (X = Br, I) are estimated from the radiative association cross sections for the temperature in the range of 10 K–15000 K. For better comparison and discussion, the radiative association rate coefficients for PBr and PI are displayed in Fig. 4 and Table 1. Due to the potential barrier against dissociation into $P(^4S) + I(^2P)$ and $P(^4S) + Br(^2P)$, the rate coefficient values increase rapidly between 10 K and 2000 K. It is concluded from Fig. 4 that the rate coefficient of PBr is higher than that of PI, mainly due to structural differences in their potential energy curves rather than polarizability alone. Although the polarizability of Br is slightly lower than that of I, the transition probability in radiative association is primarily determined by the overlap integral between the excited and ground state wavefunctions, as described by the Franck–Condon principle. As shown in Fig. 1, the ground-state potential well of PBr is deeper (0.10208 a.u.) than that of PI (0.08276 a.u.). Additionally, the $1^3\Pi$ state of PI exhibits a shallower potential well (at 4.5 Å) than that of PBr (at 2.6 Å). Consequently, PBr exhibits better wavefunction overlap between the bound and scattering states, which leads to consistently higher rate constants compared to PI. The radiative association rate constants of PBr are always larger than that of PI (Fig. 4) and their magnitudes are usually comparable to formation of other P-bearing molecules (e.g., PO, PCl^+, and PN^+) through the same mechanism.[89,90]

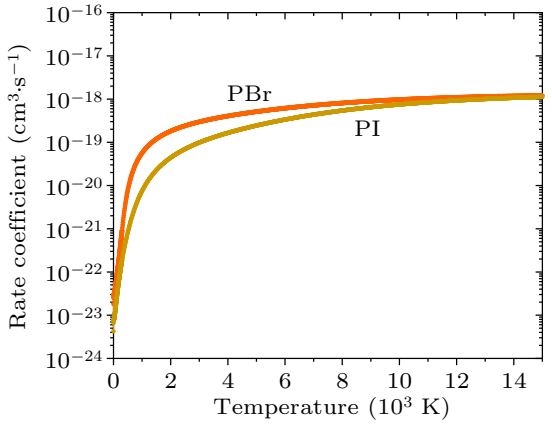


Fig. 4. Radiative association rate coefficient of PBr and PI.

Table 1. Radiative association rate coefficients of PBr and PI.

T (K)	k (cm^3·s^{-1}) (PBr)	k (cm^3·s^{-1}) (PI)
10	2.86×10^{-23}	7.73×10^{-24}
20	2.95×10^{-23}	8.00×10^{-24}
30	3.13×10^{-23}	8.66×10^{-24}
50	3.71×10^{-23}	1.07×10^{-23}
100	6.47×10^{-23}	2.10×10^{-23}
200	2.15×10^{-22}	7.13×10^{-23}
300	9.03×10^{-22}	1.87×10^{-22}
700	2.32×10^{-20}	2.44×10^{-21}
1000	5.64×10^{-20}	7.48×10^{-21}
1500	1.19×10^{-19}	2.26×10^{-20}
2000	1.81×10^{-19}	4.40×10^{-20}
2500	2.40×10^{-19}	6.96×10^{-20}
3000	2.96×10^{-19}	9.84×10^{-20}
3500	3.51×10^{-19}	1.30×10^{-19}
4000	4.04×10^{-19}	1.65×10^{-19}
4500	4.56×10^{-19}	2.03×10^{-19}
5000	5.09×10^{-19}	2.44×10^{-19}
6000	6.12×10^{-19}	3.35×10^{-19}
7000	7.12×10^{-19}	4.36×10^{-19}
8000	8.06×10^{-19}	5.42×10^{-19}
10000	9.67×10^{-19}	7.49×10^{-19}
12000	1.09×10^{-18}	9.28×10^{-19}
14000	1.17×10^{-18}	1.07×10^{-18}
15000	1.20×10^{-18}	1.12×10^{-18}

Equilibrium thermodynamics modeling of a cooling gas of solar composition predicts that bromine, iodine and phosphorus start to condense into the solid state around 293 K, 312 K, and 1248 K, respectively (e.g., Refs. [91,92]). However, P atom appears to be slightly depleted or undepleted in the diffuse clouds (e.g., Ref. [23]). Depletion of P and Br atoms should be due to freeze-out onto icy mantles of dust grains in cold astrophysical environments.[5,6,39,93] Due to relatively small rate coefficients, the RA process is likely negligible in the low temperature regions, where complex physicochemical mechanisms dominate the Br- and P-containing molecules production, which include grain disruption by energetic phenomena that releases either Br and P atoms or Br- and P-containing molecules into the gas phase.[5,6,39] However, the formation of PBr and PI by RA process may be important in a variety of astrophysical environments, as discussed above, mainly in relatively hot, low density, H- and dust-poor environments, such as ejecta of core-collapse supernovae (e.g., Ref. [70]) and Wolf–Rayet winds (e.g., Ref. [69]).

Finally, the three-parameter Arrhenius–Kooij function

$$k(T) = A\left(\frac{T}{300}\right)^{\alpha} \mathrm{e}^{-\beta/T} \tag{10}$$

is used to fit the computed rate coefficients at different temperatures, where A, α, and β are the fitting parameters. In order to fit the calculated radiative association rate coefficients more accurately, the corresponding curves were divided into several temperature ranges and adjusted separately. The fitted parameters are summarized in Table 2 for formation of PBr and PI over several temperature ranges.

Table 2. Fitting parameters of PBr and PI.

	T (K)	A (cm^3·s^{-1})	α	β (K)
PBr	1–10	2.331×10^{-23}	–0.0784	2.7057
	10–30	4.882×10^{-23}	0.2334	–2.6353
	30–100	2.032×10^{-22}	1.4863	–47.5537
	100–300	8.349×10^{-23}	6.4567	–710.1805
	300–3000	1.388×10^{-19}	0.5556	1570.8715
	3000–8000	5.538×10^{-20}	0.8483	838.6556
	8000–15000	9.797×10^{-18}	–0.3528	10763.5643
PI	1–10	4.865×10^{-24}	–0.1645	1.0652
	10–30	1.604×10^{-23}	0.3263	–3.8522
	30–100	8.236×10^{-23}	1.7515	–54.5274
	100–300	9.258×10^{-23}	3.2282	–209.2252
	300–3000	1.025×10^{-20}	1.2449	1809.7764
	3000–8000	3.737×10^{-21}	1.5527	938.1230
	8000–15000	1.441×10^{-17}	–0.3673	16673.1226

4. Summary

Using accurate electronic *ab inito* data, we have calculated the cross sections for the radiative association of P and X (X = Br and I) atoms to form PBr and PI molecules employing a fully quantum mechanical approach. For PBr and PI, the molecule-forming transitions were assumed dominantly to occur through the $1^3\Pi$ state followed by radiative transition to the ground $X^3\Sigma^-$ state. Rate coefficients have been obtained from the cross sections for temperature in the range of 10 K–15000 K. The rate constant values of PBr increase from about 2.86×10^{-23} cm^3·s^{-1} at 10 K to about 1.20×10^{-18} cm^3·s^{-1} at 15000 K, and those of PI range from about 7.73×10^{-24} cm^3·s^{-1} at 10 K to about 1.12×10^{-18} cm^3·s^{-1} at 15000 K. The computed radiative association rate coefficients for PBr and PI are suitable for applicability in a variety of environments, mainly in relatively hot, low density, H- and dust-poor environments.

The formation of phosphorus monobromide (PBr) and phosphorus monoiodide (PI) radicals through radiative association expands our understanding of phosphorus chemistry in space and offers insights into the role of halogens in the astrochemical environments. Further studies would be necessary to fully understand the role of these molecules in space, their formation, distribution, and astrophysical significance.

Acknowledgements

Project supported by the Science and Technology Development Plan Project of Jilin Province, China (Grant No. YDZJ202201ZYTS314), the National Natural Science Foundation of China (Grant Nos. 12274178 and 11874177), and the support from the High Performance Computing Center (HPCC) of Jilin University and the High-Performance Computing Cluster Tiger@ IAMP. Finally, we would also like to thank Professors Yong Wu and Jianguo Wang for their help.

References

[1] Asplund M, Amarsi A M and Grevesse N 2021 *A & A* **653** A141
[2] Saiz-Lopez A, Plane J, Baker A, Carpenter L, Von Glasow R, Gómez Martín J, McFiggans G and Saunders R 2012 *Chem. Rev.* **112** 1773
[3] Wang S, McNamara S M, Moore C W, Obrist D, Steffen A, Shepson P B, Staebler R M, Raso A R W and Pratt K A 2019 *Proc. Natl. Acad. Sci. USA* **116** 14479
[4] Keber T, Bönisch H, Hartick C, Hauck M, Lefrancois F, Obersteiner F, Ringsdorf A, Schohl N, Schuck T, Hossaini R, Graf P, Jöckel P and Engel A 2020 *Atmos. Chem. Phys.* **20** 4105
[5] Dhooghe F, De Keyser J, Altwegg K, Briois C, Balsiger H, Berthelier J J, Calmonte U, Cessateur G, Combi M R, Equeter E, Fiethe B, Fray N, Fuselier S, Gasc S, Gibbons A, Gombosi T, Gunell H, Hässig M, Hilchenbach M, Le Roy L, Maggiolo R, Mall U, Marty B, Neefs E, Rème H, Rubin M, Sémon T, Tzou C Y and Wurz P 2017 *MNRAS* **472** 1336
[6] Ligterink N F W and Kama M 2018 *A & A* **614** A112
[7] Chayer P, Vennes S, Dupuis J and Kruk J W 2005 *ApJ* **630** L169
[8] Werner K, Rauch T, Ringat E and Kruk J W 2012 *ApJ* **753** L7
[9] Rauch T, Quinet P, Knörzer M, Hoyer D, Werner K, Kruk J W and Demleitner M 2017 *A & A* **606** A105
[10] Hoyer D, Rauch T, Werner K and Kruk J W 2018 *A & A* **612** A62
[11] Löbling L, Maney M A, Rauch T, Quinet P, Gamrath S, Kruk J W and Werner K 2020 *MNRAS* **492** 528
[12] Bidelman W P 2005 *ASP Conf. Ser.* **336** 309
[13] Castelli F and Hubrig S 2004 *A & A* **425** 263
[14] Cowley C R and Wahlgren G M 2006 *A & A* **447** 681

[15] Sharpee B, Zhang Y, Williams R, Pellegrini E, Cavagnolo K, Baldwin J A, Phillips M and Liu X W 2007 *ApJ* **659** 1265
[16] Madonna S, García-Rojas J, Sterling N C, Delgado-Inglada G, Mesa-Delgado A, Luridiana V, Roederer I U and Mashburn A L 2017 *MNRAS* **471** 1341
[17] Madonna S, Bautista M, Dinerstein H L, Sterling N C, García-Rojas J, Kaplan K F, Rubio-Díez M M, Castro-Rodríguez N and Garzón F 2018 *ApJ* **861** L8
[18] Werner K, Rauch T, Knörzer M and Kruk J W 2018 *A & A* **614** A96
[19] Gardner E, Lehto H J, Lehto K, Fray N, Bardyn A, Lönnberg T, Merouane S, Isnard R, Cottin H, Hilchenbach M and The Cosima Team 2020 *MNRAS* **499** 1870
[20] Flynn G J, Bleuet P, Borg J, *et al.* 2006 *Science* **314** 1731
[21] Kissel J and Krueger F R 1987 *Nature* **328** 117
[22] Lewis J A and Jones R H 2016 *Meteorit. Planet. Sci.* **51** 1886
[23] Lebouteiller V, Kuassivi and Ferlet R 2005 *A & A* **443** 509
[24] Molaro P, Levshakov S A, D'Odorico S, Bonifacio P and Centurión M 2001 *ApJ* **549** 90
[25] Otsuka M, Meixner M, Riebel D, Hyung S, Tajitsu A and Izumiura H 2011 *ApJ* **729** 39
[26] Koo B C, Lee Y H, Moon D S, Yoon S C and Raymond J C 2013 *Science* **342** 1346
[27] Altwegg K, Balsiger H, Bar-Nun A, Berthelier J J, Bieler A, Bochsler P, Briois C, Calmonte U, Combi M R, Cottin H, De Keyser J, Dhooghe F, Fiethe B, Fuselier S A, Gasc S, Gombosi T I, Hansen K C, Haessig M, Ja ckel A, Kopp E, Korth A, Le Roy L, Mall U, Marty B, Mousis O, Owen T, Reme H, Rubin M, Semon T, Tzou C Y, Waite J H and Wurz P 2016 *Sci. Adv.* **2** e1600285
[28] Rivilla V M, Drozdovskaya M N, Altwegg K, Caselli P, Beltrán M T, Fontani F, van der Tak F F S, Cesaroni R, Vasyunin A, Rubin M, Lique F, Marinakis S, Testi L, Rosina Team, Balsiger H, Berthelier J J, de Keyser J, Fiethe B, Fuselier S A, Gasc S, Gombosi T I, Sémon T and Tzou C Y 2020 *MNRAS* **492** 1180
[29] Caffau E, Andrievsky S, Korotin S, Origlia L, Oliva E, Sanna N, Ludwig H G and Bonifacio P 2016 *A & A* **585** A16
[30] Maas Z G, Pilachowski C A and Cescutti G 2017 *ApJ* **841** 108
[31] Masseron T, García-Hernández D A, Santoveña R, Manchado A, Zamora O, Manteiga M and Dafonte C 2020 *Nat. Commun.* **11** 3759
[32] Guelin M, Cernicharo J, Paubert G and Turner B E 1990 *A & A* **230** L9
[33] Cernicharo J, Guélin M and Kahane C 2000 *AASS* **142** 181
[34] Agúndez M, Cernicharo J and Guélin M 2007 *ApJ* **662** L91
[35] Tenenbaum E D, Woolf N J and Ziurys L M 2007 *ApJ* **666** L29
[36] Halfen D T, Clouthier D J and Ziurys L M 2008 *ApJ* **677** L101
[37] Agúndez M, Cernicharo J, Decin L, Encrenaz P and Teyssier D 2014 *ApJ* **790** L27
[38] Agúndez M, Cernicharo J and Guélin M 2014 *A & A* **570** A45
[39] Koelemay L A, Burton M A, Singh A P, Sheridan P M, Bernal J J and Ziurys L M 2022 *ApJ* **940** L11
[40] Turner B E and Bally J 1987 *ApJ* **321** L75
[41] Ziurys L M 1987 *ApJ* **321** L81
[42] Lefloch B, Vastel C, Viti S, Jimenez-Serra I, Codella C, Podio L, Ceccarelli C, Mendoza E, Lepine J R D and Bachiller R 2016 *MNRAS* **462** 3937
[43] Rivilla V M, Fontani F, Beltrán M T, Vasyunin A, Caselli P, Martín-Pintado J and Cesaroni R 2016 *ApJ* **826** 161
[44] Rivilla V M, García De La Concepción J, Jiménez-Serra I, Martín-Pintado J, Colzi L, Tercero B, Megías A, López-Gallifa Á, Martínez-Henares A, Massalkhi S, Martín S, Zeng S, De Vicente P, Rico-Villas F, Requena-Torres M A and Cosentino G 2022 *Front. Astron. Space Sci.* **9** 829288
[45] Koelemay L A, Gold K R and Ziurys L M 2023 *Nature* **623** 292
[46] Scibelli S, Megías A, Jiménez-Serra I, Shirley Y, Bergner J, Ferrer Asensio J, Garrod R T, Bonfand M and Pokorny-Yadav A 2025 *ApJL* **985** L25
[47] Haasler D, Rivilla V M, Martín S, Holdship J, Viti S, Harada N, Mangum J, Sakamoto K, Muller S, Tanaka K, Yoshimura Y, Nakanishi K, Colzi L, Hunt L, Emig K L, Aladro R, Humire P, Henkel C and van der Werf P 2022 *A & A* **659** A158
[48] Larson H P, Treffers R R and Fink U 1977 *ApJ* **211** 972
[49] Bregman J D, Lester D F and Rank D M 1975 *ApJ* **202** L55
[50] Remick K A and Helmann J D 2023 *Adv. Microb. Physiol.* **82** 1
[51] Woosley S E and Weaver T A 1995 *ApJSS* **101** 181
[52] Cescutti G, Matteucci F, Caffau E and François P 2012 *A & A* **540** A33
[53] Takahashi K, Yoshida T and Umeda H 2018 *ApJ* **857** 111
[54] Prantzos N, Abia C, Limongi M, Chieffi A and Cristallo S 2018 *MNRAS* **476** 3432
[55] Farmer R, Laplace E, Ma J z, de Mink S E and Justham S 2023 *ApJ* **948** 111
[56] Karakas A I 2010 *MNRAS* **403** 1413
[57] Doherty C L, Gil-Pons P, Lau H H B, Lattanzio J C, Siess L and Campbell S W 2014 *MNRAS* **441** 582
[58] Iwamoto K, Brachwitz F, Nomoto K, Kishimoto N, Umeda H, Hix W R and Thielemann F K 1999 *AASS* **125** 439
[59] Keegans J D, Pignatari M, Stancliffe R J, Travaglio C, Jones S, Gibson B K, Townsley D M, Miles B J, Shen K J and Few G 2023 *ApJSS* **268** 8
[60] José J and Hernanz M 1998 *ApJ* **494** 680
[61] Downen L N, Iliadis C, José J and Starrfield S 2013 *ApJ* **762** 105
[62] Davila N, Bojazi M J and Meyer B S 2019 *AIP Conf. Proc* **2076** 030005
[63] Banerjee P, Wu M R and S K J 2022 *MNRAS* **512** 4948
[64] Chen M H and Liang E W 2024 *MNRAS* **527** 5540
[65] Cescutti G, Hirschi R, Nishimura N, Hartogh J W d, Rauscher T, Murphy A S J and Cristallo S 2018 *MNRAS* **478** 4101
[66] Hampel M, Karakas A I, Stancliffe R J, Meyer B S and Lugaro M 2019 *ApJ* **887** 11
[67] Swings P 1942 *ApJ* **95** 270
[68] Liu W and Dalgarno A 1994 *ApJ* **428** 769
[69] Cherchneff I, Le Teuff Y H, Williams P M and Tielens A G G M 2000 *A & A* **357** 572
[70] Ono M, Nozawa T, Nagataki S, Kozyreva A, Orlando S, Miceli M and Chen K J 2024 *ApJS* **271** 33
[71] Pontefract M and Rawlings J M C 2004 *MNRAS* **347** 1294
[72] Derdzinski A M, Metzger B D and Lazzati D 2017 *MNRAS* **469** 1314
[73] Glassgold A E, Mamon G A and Huggins P J 1991 *ApJ* **373** 254
[74] Cherchneff I 2012 *A & A* **545** A12
[75] Millar T J, Walsh C, Van de Sande M and Markwick A J 2024 *A & A* **682** A109
[76] Stancil P C, Kirby K, Gu J P, Hirsch G, Buenker R J and Sannigrahi A B 2000 *AASS* **142** 107
[77] Antipov S V, Gustafsson M and Nyman G 2013 *MNRAS* **430** 946
[78] Wei H and Liu X 2018 *Chin. Phys. B* **27** 123101
[79] Herzberg G 1950 *Molecular spectra and molecular structure*, Vol. 1: Spectra of diatomic molecules
[80] Zhang X, Liu X, Liang G, Li R, Xu H and Yan B 2016 *JQSRT* **168** 66
[81] Zhang X, Yan P, Li R, Gai Z, Liang G, Xu H and Yan B 2016 *JQSRT* **180** 154
[82] Zhang X, Liu X, Liang G, Shi D, Li R, Liu X, Xu H and Yan B 2015 *Mol. Phys.* **113** 3312
[83] Lin X H, Liang G Y, Wang J G, Peng Y G, Shao B, Li R and Wu Y 2019 *Chin. Phys. B* **28** 053101
[84] Chang T Y 1967 *Rev. Mod. Phys.* **39** 911
[85] London F 1937 *Trans. Faraday Soc.* **33** 8b–26
[86] NIST 2025 Atomic spectra database levels form accessed: 2025-06-13
[87] Miller T M and Bederson B 1978 *Adv. Atom. Mol. Opt. Phy.* **13** 1
[88] Shevelko V P and Vinogradov A V 1979 *Phys. Scr.* **19** 275
[89] Chen Y, Lin X, Xiao L, Li Z, Zhang S, Cheng Y, Wu Y and Yan B 2024 *Front. Astron. Space Sci.* **11** 1335464
[90] Wei Q, Chen Y, de Almeida A A, Andreazza C M and Yan B 2025 *A & A* **A233** 9
[91] Lodders K 2003 *ApJ* **591** 1220
[92] Lodders K and Fegley Jr B 2023 *Geochemistry* **83** 125957
[93] Chantzos J, Rivilla V M, Vasyunin A, Redaelli E, Bizzocchi L, Fontani F and Caselli P 2020 *A & A* **633** A54